2013 European Control Conference (ECC)
July 17-19, 2013, Zürich, Switzerland.

Stable Region of Gravity Position of Object Grasped by Virtual Springs

Akira Nakashima[1] and Yoshikazu Hayakawa[1]

Abstract—**This paper considers the stable grasp in the sense of quasi-statistics, i.e., an object is grasped by a multi-fingered robot hand, where each finger is regarded as a virtual 3D linear spring. The stability analysis is to find a condition under which the equilibrium can be restored after any small perturbations of the object's position and orientation. The paper derives a necessary and sufficient condition for the grasp to be stable in terms of relations among the stiffness parameters, the contact points, and the object's COG. By using this result, a region of the object's COG can be clarified which guarantees the stable grasp.**

I. Introduction

Many researchers have tried to introduce robots into human's daily life environments, where the robots are aimed to do various tasks instead of humans. Then, multi-fingered robot hands are effective as end-effectors because they have capability to grasp and manipulate variously-shaped objects with multi contacts and multi joints. Especially, the grasp has to be established primarily and eternally before and awhile manipulation, so it is very important that the grasp is stable. The stable grasp has been dealt with from the viewpoints of the statics, dynamics and quasi-statics. The studies of these viewpoints are briefly reviewed and some of them are surveyed in [1], [2], [3].

The stable grasp in the sense of the statics means the analysis and optimization of the factors, i.e., the grasping forces, the contact points and the configurations of the object and fingers. Some of the criteria in the optimizations are the friction and torque limitations [4]; a safety factor to prevent the break of the object [5]; a force decomposition based on a clear physical meaning [6]; the Force-Closure, e.g. [7], [8]. All the factors are considered in [9] with sets of required external forces and acceleration. An application for grasping assembling parts by a four-fingered robot hand by optimizing all the factors is shown in [10].

The stable grasp in the sense of the dynamics has been considered from the viewpoints of the computed torque law and the Lyapunov theory. The first one is a major control method in robotics and was initially used for the grasp and manipulation, e.g., [11], [12] and [13]. The second one is a major stability theory in the control theory and has been studied, e.g., [14], [15], [16] and [17]. Control methods based on the concept of stability on a manifold were proposed in [18] and a 3D manipulation case was discussed in [19]. A port-Hamiltonian approach was applied to the soft-finger manipulation with cases of contact and non-contact in [20].

The stable grasp in the sense of the quasi-statics is discussed based on the *stiffness-effect* [21], which is the resultant force and moment due to the unbalanced grasping forces when the grasped object is perturbed from its equilibrium point. Hanafusa and Asada [22] considered the grasp by fingers, each of which is assumed to be one degree of freedom (DOF) linear spring. They derived that an equilibrium of the grasp is stable if and only if it is a strict local minimum of the elastic potential energy due to the fingers. This result was extended to the grasp with the two DOF springs [23], [24]. The case in 3D space was discussed in [25], [26]. The effects of the rolling contact and the curvatures of the fingers and object were studied in [26], [27], [28]. The contribution of the structural and actuational elements in a grasp to the stiffness was identified in [21]. The stiffness between the fingers were considered as well as the stiffness of the fingers in [29]. It is shown there that the stiffnesses and contact points can be obtained, under which the grasp is guaranteed to be stable when the object parameters are given. Therefore, this type of the grasp is feasible since the stiffness can be realized by compliance or impedance controls, e.g., [29], [30]. However, the *gravity effect* is ignored in the previous studies above though it can destabilize the grasp. In fact, it is easy to image that the grasp may be unstable in the case that the center of gravity (COG) is located above a center of rotational perturbation. Svinin et al. [31] analyzed the effect of the gravity for the grasped object with frictional and constant grasping forces, which is not a virtual spring model.

This paper considers the stable grasp from viewpoint of quasi-statics where a multi-fingered robot grasps an object by point contact. In the same way as the previous researches shown above, it is assumed here that each finger's grasping is regarded as a linear spring with three-DOF stiffness. But, unlike the previous researches, this paper considers the gravity effect explicitly. The main contribution of the paper is to derive a necessary and sufficient condition for the multi-fingered grasp to be stable under the gravity effect in terms of relations among the stiffness parameters, the contact points, and the object's COG. This result modifies the authors' previous ones [30], [32] by correcting some misunderstandings as well as relaxing some conditions. By using the main result, it is easy to see where the object's COG should be located to guarantee the stable grasp. Furthermore, this observation shows that it is possible under a certain condition that no matter where the object's COG is located, the grasp is stable.

II. Preliminaries

A. System Configuration

Consider an equilibrium situation of an object grasped by the ith finger at the ith contact point C_i $(i = 1, \cdots, n)$ as

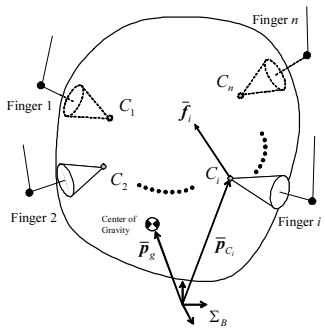

Fig. 1. An Object grasped by n fingers.

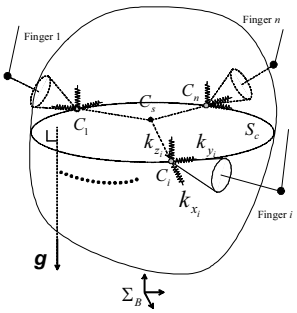

Fig. 3. Assumptions for the equilibrium.

shown in Fig. 1, where Σ_B is the inertial frame of reference, $\bar{\boldsymbol{p}}_{C_i} \in \mathbb{R}^3$ is the ith contact point, $\bar{\boldsymbol{p}}_g \in \mathbb{R}^3$ is the position of the COG, and $\bar{\boldsymbol{f}}_i \in \mathbb{R}^3$ is the grasping force at C_i. Note that the variables with the bars "$^-$" denote the ones at the equilibrium. The equilibrium situation means that the forces and moments exerted on the object are balanced. In this study, the stability of the grasp is investigated when the object is perturbed with respect to the position and orientation from its equilibrium.

We make the following assumptions for the contact points C_i's and the grasping forces $\boldsymbol{f}_i$'s:

Assumption 1: All the contact points C_i's are located in a same plane S_c as shown in Fig. 2 (a). The contact type is the point contact and the contact locations are fixed on the object.

Assumption 2: The ith finger is controlled by a compliance control method. It is assumed that the ith finger behaves as the 3D virtual translational spring $(k_{x_i}, k_{y_i}, k_{z_i})$ as shown in Fig. 2 (b). The virtual walls W_{x_i}, W_{y_i} and W_{z_i} are perpendicular to each other. The spring k_{x_i} is attached to C_i as well as W_{x_i}, where k_{x_i} is always kept to be perpendicular to W_{x_i} even if C_i moves. The springs k_{y_i} and k_{z_i} follow the same behavior as k_{x_i}.

We also make the following assumptions for the equilibrium:

Assumption 3: The plane S_c coincides with the horizontal plane at the equilibrium as shown in Fig. 3.

Assumption 4: The elongations of all the springs k_{x_i}'s intersect at one point C_s in the plane S at the equilibrium as shown in Fig. 3.

Without loss of generality, the springs k_{z_i}'s are set vertically and the springs k_{y_i}'s are set for the spring $(k_{x_i}, k_{y_i}, k_{z_i})$ to be the right-handed coordinate system.

From all the assumptions, the equilibrium situation of the grasp is expressed by Fig. 4. Now we set the reference frame Σ_B to C_s. The object frame Σ_O is fixed to the object at C_s to coincide with Σ_B. The ith spring frame Σ_{S_i} is fixed with respect to Σ_B at C_i and its x-, y- and z-axes are set along the springs k_{x_i}, k_{y_i} and k_{z_i} respectively.

Associated with the ith contact point C_i, the contact parameter is defined as $(\bar{r}_i, \bar{\alpha}_i, \bar{\beta}_i)$, where $\bar{r}_i$ is the distance, $\bar{\alpha}_i$ and $\bar{\beta}_i = \frac{\pi}{2}$ are the angles from the x- and y-axes respectively. Similarly, associated with the the COG, the gravity parameter is defined as $(\bar{r}_g, \bar{\alpha}_g, \bar{\beta}_g)$, which denote the distance, the angles from the x- and y-axes respectively. Then, the ith contact point C_i and the COG are expressed by $\bar{\boldsymbol{p}}_{C_i} = \bar{r}_i[C_{\bar{\alpha}_i},\ S_{\bar{\alpha}_i},\ 0]^{\mathrm{T}}$ and $\bar{\boldsymbol{p}}_g = \bar{r}_g[S_{\bar{\beta}_g}C_{\bar{\alpha}_g},\ S_{\bar{\beta}_g}S_{\bar{\alpha}_g},\ C_{\bar{\beta}_g}]^{\mathrm{T}}$ in Σ_B respectively, where C_α and S_α denote $\cos\alpha$ and $\sin\alpha$ respectively as well as C_β and S_β.

The spring k_{x_i} has the coefficient k_{x_i} and the displacement δ_{x_i} as well as the springs k_{y_i} and k_{z_i} as shown in Fig. 2 (b). The spring displacements are denoted by $\boldsymbol{\delta}_i := [\delta_{x_i}\ \delta_{y_i}\ \delta_{z_i}]^{\mathrm{T}} \in \mathbb{R}^3$. Note that the positive and negative

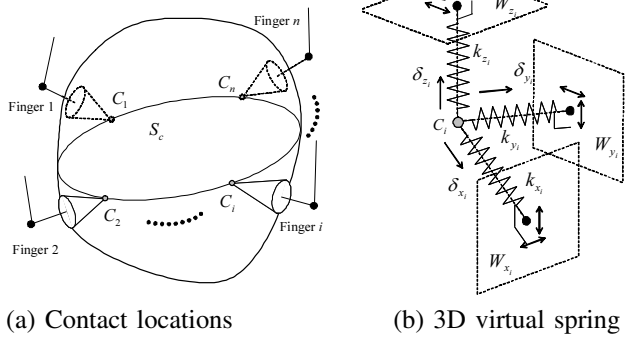

(a) Contact locations (b) 3D virtual spring

Fig. 2. Assumptions for the contact points and grasping forces.

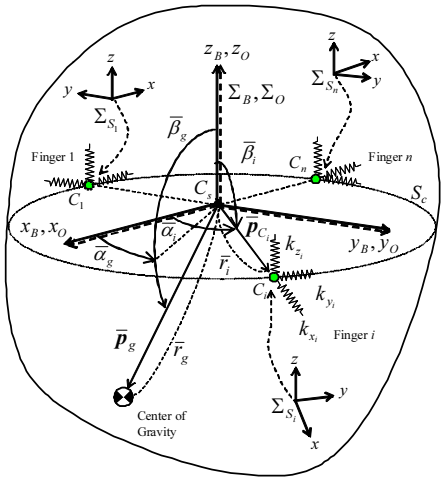

Fig. 4. An object grasped by virtual spring fingers.

values of $\boldsymbol{\delta}_i$ represent the compression and extension from the natural thinning.

The ith grasping force $\bar{\boldsymbol{f}}_i$ is given by $\bar{\boldsymbol{f}}_i = -\boldsymbol{R}_{S_i}\boldsymbol{K}_i\bar{\boldsymbol{\delta}}_i$. $\bar{\boldsymbol{\delta}}_i := [\bar{\delta}_{x_i}\ \bar{\delta}_{y_i}\ \bar{\delta}_{z_i}]^{\mathrm{T}}$ represents the spring displacements at the equilibrium. $\boldsymbol{R}_{S_i} := \boldsymbol{R}_Z(\bar{\alpha}_i)$ is the rotation matrix of Σ_{S_i} with respect to Σ_B, where $\boldsymbol{R}_Z \in \mathbb{R}^{3\times3}$ is the rotation matrix about z-axis. $\boldsymbol{K}_i := \mathrm{diag}(k_{x_i}, k_{y_i}, k_{z_i})$ is the stiffness matrix of the ith spring.

The perturbation to the object from the equilibrium is represented by $\boldsymbol{u} := [\,\boldsymbol{p}_O^{\mathrm{T}}\ \ \boldsymbol{\phi}_O^{\mathrm{T}}\,]^{\mathrm{T}} \in \mathbb{R}^6$, where $\boldsymbol{p}_O,\ \boldsymbol{\phi}_O \in \mathbb{R}^3$ denote the position and the roll-pitch-yaw angles of the rotation matrix $\boldsymbol{R}_O \in \mathbb{R}^{3\times3}$ of Σ_O with respect to Σ_B.

B. Stability Conditions

For the grasp, we define the stability when the object is perturbed from the equilibrium with any small perturbation $\boldsymbol{u} \in \mathbb{R}^6$. The potential energy of the grasp is given by

$$U(\boldsymbol{u}) = \frac{1}{2}\textstyle\sum_{i=1}^{n}\boldsymbol{\delta}_i(\boldsymbol{u})^{\mathrm{T}}\boldsymbol{K}_i\boldsymbol{\delta}_i(\boldsymbol{u}) - \boldsymbol{p}_g(\boldsymbol{u})^{\mathrm{T}}m\boldsymbol{g}, \quad (1)$$

where

$$\boldsymbol{p}_g(\boldsymbol{u}) = \boldsymbol{R}_O(\boldsymbol{\phi}_O)\bar{\boldsymbol{p}}_g + \boldsymbol{p}_O, \quad (2)$$

$$\boldsymbol{\delta}_i(\boldsymbol{u}) = \boldsymbol{R}_{S_i}^{-1}((\boldsymbol{R}_O(\boldsymbol{\phi}_O) - \boldsymbol{I}_3)\bar{\boldsymbol{p}}_{C_i} + \boldsymbol{p}_O) + \bar{\boldsymbol{\delta}}_i. \quad (3)$$

Suppose that $U(\boldsymbol{u})$ is differentiable twice with respect to $\boldsymbol{u}$. The grasp is stable at $\boldsymbol{u} = \boldsymbol{u}_e$ if the following conditions hold [22]:

$$\nabla U(\boldsymbol{u}_e) = \boldsymbol{0}, \quad \nabla^2 U(\boldsymbol{u}_e) \succ 0. \quad (4)$$

The first condition of (4) denotes that $\boldsymbol{u}_e$ is an equilibrium and the second one denotes that it is stable.

In this paper, we consider that $\boldsymbol{u}_e$ is equal to $\boldsymbol{0}$. The first condition of (4) with $\boldsymbol{u}_e = \boldsymbol{0}$ leads to

$$\textstyle\sum_{i=1}^{n}\bar{\boldsymbol{f}}_i + m\boldsymbol{g} = \boldsymbol{0}, \quad (5)$$

$$\textstyle\sum_{i=1}^{n}\bar{\boldsymbol{p}}_{C_i} \times \bar{\boldsymbol{f}}_i + \bar{\boldsymbol{p}}_g \times m\boldsymbol{g} = \boldsymbol{0}, \quad (6)$$

where m is the mass of the object and $\boldsymbol{g} := [0\ 0\ -g]^{\mathrm{T}} \in \mathbb{R}^3$ with $g = 9.8$ [m/s^2] is the gravity vector. Now, the second condition of (4) will be investigated below. The matrix $\nabla^2 U(\boldsymbol{0}) \in \mathbb{R}^{6\times6}$ is calculated as

$$\nabla^2 U(\boldsymbol{0}) = \begin{bmatrix}\boldsymbol{K}_{pp} & \boldsymbol{K}_{p\phi}\\ \boldsymbol{K}_{p\phi}^{\mathrm{T}} & \boldsymbol{K}_{\phi\phi}\end{bmatrix}, \quad (7)$$

where

$$\boldsymbol{K}_{\phi\phi} := M\begin{bmatrix}a - C_{\bar{\beta}_g} & -d & 0\\ -d & b - C_{\bar{\beta}_g} & 0\\ 0 & 0 & c\end{bmatrix}, \quad (8)$$

$$\boldsymbol{K}_{p\phi} := \textstyle\sum_{i=1}^{n}\boldsymbol{R}_{S_i}\boldsymbol{K}_i\boldsymbol{R}_{S_i}^{\mathrm{T}}[\bar{\boldsymbol{p}}_{C_i}\times]^{\mathrm{T}} = M\begin{bmatrix}0 & 0 & e\\ 0 & 0 & f\\ g & h & 0\end{bmatrix} \quad (9)$$

$$\boldsymbol{K}_{pp} := \textstyle\sum_{i=1}^{n}\boldsymbol{R}_{S_i}\boldsymbol{K}_i\boldsymbol{R}_{S_i}^{\mathrm{T}} = M\begin{bmatrix}q & r & 0\\ r & s & 0\\ 0 & 0 & p\end{bmatrix}. \quad (10)$$

Note that $[\bar{\boldsymbol{p}}_{C_i}\times] \in \mathbb{R}^{3\times3}$ is the skew-symmetric matrix equivalent to the cross product of $\bar{\boldsymbol{p}}_{C_i}$. The components a to s are defined as $a := A/M, \cdots, s := S/M$, where the capitals A to S and M are given by

$$\begin{aligned}
A &:= \textstyle\sum_{i=1}^{n}\left\{(k_{z_i}\bar{r}_i - k_{x_i}\bar{\delta}_{x_i})S_{\bar{\alpha}_i} - k_{y_i}\bar{\delta}_{y_i}C_{\bar{\alpha}_i}\right\}\bar{r}_i S_{\bar{\alpha}_i}\\
B &:= \textstyle\sum_{i=1}^{n}\left\{(k_{z_i}\bar{r}_i - k_{x_i}\bar{\delta}_{x_i})C_{\bar{\alpha}_i} + k_{y_i}\bar{\delta}_{y_i}S_{\bar{\alpha}_i}\right\}\bar{r}_i C_{\bar{\alpha}_i}\\
C &:= \textstyle\sum_{i=1}^{n}(k_{y_i}\bar{r}_i - k_{x_i}\bar{\delta}_{x_i})\bar{r}_i\\
D &:= \textstyle\sum_{i=1}^{n}\left\{(k_{z_i}\bar{r}_i - k_{x_i}\bar{\delta}_{x_i})C_{\bar{\alpha}_i} + k_{y_i}\bar{\delta}_{y_i}S_{\bar{\alpha}_i}\right\}\bar{r}_i S_{\bar{\alpha}_i}\\
E &:= \textstyle\sum_{i=1}^{n}k_{y_i}\bar{r}_i S_{\bar{\alpha}_i}, \quad F := \textstyle\sum_{i=1}^{n}k_{y_i}\bar{r}_i C_{\bar{\alpha}_i}\\
G &:= \textstyle\sum_{i=1}^{n}k_{z_i}\bar{r}_i S_{\bar{\alpha}_i}, \quad H := \textstyle\sum_{i=1}^{n}k_{z_i}\bar{r}_i C_{\bar{\alpha}_i}\\
Q &:= \textstyle\sum_{i=1}^{n}(k_{x_i}C_{\bar{\alpha}_i}^2 + k_{y_i}S_{\bar{\alpha}_i}^2), R := \textstyle\sum_{i=1}^{n}(k_{x_i} - k_{y_i})S_{\bar{\alpha}_i}C_{\bar{\alpha}_i}\\
S &:= \textstyle\sum_{i=1}^{n}(k_{x_i}S_{\bar{\alpha}_i}^2 + k_{y_i}C_{\bar{\alpha}_i}^2),\ P := \textstyle\sum_{i=1}^{n}k_{z_i}\\
M &:= \bar{r}_g mg.
\end{aligned}$$

$\boldsymbol{K}_{pp} \in \mathbb{R}^{3\times3}$ represents the stiffness effect from the position to the translational force. $\boldsymbol{K}_{p\phi} \in \mathbb{R}^{3\times3}$ represents the coupling between the position and orientation. $\boldsymbol{K}_{\phi\phi} \in \mathbb{R}^{3\times3}$ represents the stiffness effect from the orientation to the moment. M is called as the *gravity effect* in this paper.

Since $\nabla^2 U(\boldsymbol{0})$ is the symmetric matrix, $\nabla^2 U(\boldsymbol{0})$ is positive definite if and only if

$$\boldsymbol{K}_{pp} \succ 0, \quad (11)$$

$$\boldsymbol{K}_{\phi\phi} - \boldsymbol{K}_{p\phi}^{\mathrm{T}}\boldsymbol{K}_{pp}^{-1}\boldsymbol{K}_{p\phi} \succ 0 \quad (12)$$

from Schur's complement [33]. Since every $\boldsymbol{K}_i$ is positive definite, it is evident from (10) that (11) always holds. Then, the stability analysis is shown by considering (12).

III. Stability Analysis

A. Problem Setting

With (9) and (10), $\boldsymbol{K}_{p\phi}^{\mathrm{T}}\boldsymbol{K}_{pp}^{-1}\boldsymbol{K}_{p\phi}$ is calculated as

$$\boldsymbol{K}_{p\phi}^{\mathrm{T}}\boldsymbol{K}_{pp}^{-1}\boldsymbol{K}_{p\phi} = M\begin{bmatrix}p^{-1}\boldsymbol{\xi}\boldsymbol{\xi}^{\mathrm{T}} & \boldsymbol{0}_{2\times1}\\ \boldsymbol{0}_{1\times2} & \boldsymbol{\eta}^{\mathrm{T}}\tilde{\boldsymbol{K}}_{pp}'^{-1}\boldsymbol{\eta}\end{bmatrix}, \quad (13)$$

where $\tilde{\boldsymbol{K}}_{pp}' := \left[\begin{smallmatrix}q & r\\ r & s\end{smallmatrix}\right]$, $\boldsymbol{\xi} := [g\ h]^{\mathrm{T}}$, $\boldsymbol{\eta} := [e\ f]^{\mathrm{T}}$. Thus, $\boldsymbol{K}_{\phi\phi} - \boldsymbol{K}_{p\phi}^{\mathrm{T}}\boldsymbol{K}_{pp}^{-1}\boldsymbol{K}_{p\phi}$ in (12) is given by

$$\boldsymbol{K}_{\phi\phi} - \boldsymbol{K}_{p\phi}^{\mathrm{T}}\boldsymbol{K}_{pp}^{-1}\boldsymbol{K}_{p\phi} = M\begin{bmatrix}\tilde{a} - x & -\tilde{d} & 0\\ -\tilde{d} & \tilde{b} - x & 0\\ 0 & 0 & \tilde{c}\end{bmatrix}, \quad (14)$$

where $x := C_{\bar{\beta}_g}$ and

$$\begin{cases}\tilde{a} := a - p^{-1}g^2, & \tilde{b} := b - p^{-1}h^2\\ \tilde{c} := c - \boldsymbol{\eta}^{\mathrm{T}}\tilde{\boldsymbol{K}}_{pp}'^{-1}\boldsymbol{\eta}, & \tilde{d} := d + p^{-1}gh\end{cases}. \quad (15)$$

From the Sylvester's criterion for the condition (12), (12) holds if and only if all the following principal minors of (14) are positive:

$$\tilde{f}_1(x) := -x + \tilde{a} \quad (16)$$

$$\tilde{f}_2(x) := (x - \tilde{a})(x - \tilde{b}) - \tilde{d}^2 \quad (17)$$

$$\tilde{f}_3(x) := \tilde{c}\tilde{f}_2(x), \quad (18)$$

where $\tilde{f}_j(x)$ $(j = 1, 2, 3)$ is the jth principal minor.

For the formulation of the stability problem, we define the following sets with respect to x:

$$\mathcal{R}_0 := \{\ x \mid -1 \le x \le 1\ \}, \tag{19}$$

$$\tilde{\mathcal{R}}_j := \{\ x \mid \tilde{f}_j(x) > 0\ \}, \tag{20}$$

$$\tilde{\mathcal{R}}_{01} := \mathcal{R}_0 \cap \tilde{\mathcal{R}}_1, \tilde{\mathcal{R}}_{012} := \tilde{\mathcal{R}}_{01} \cap \tilde{\mathcal{R}}_2, \tilde{\mathcal{R}}_{0123} := \tilde{\mathcal{R}}_{012} \cap \tilde{\mathcal{R}}_3. \tag{21}$$

Then, the stability problem is formulated with respect to the position of the COG:

Problem 1: Suppose that the contact parameters $(\bar{r}_i, \bar{\alpha}_i)$, the stiffness coefficients $(k_{x_i}, k_{y_i}, k_{z_i})$ and the initial spring displacements $\bar{\boldsymbol{\delta}}_i = [\bar{\delta}_{x_i}\ \bar{\delta}_{y_i}\ \bar{\delta}_{z_i}]^{\mathrm{T}}$ are given to satisfy (5) and (6). Find a necessary and sufficient condition on x for the equilibrium $\boldsymbol{u} = \boldsymbol{0}$ to be stable.

B. Analysis Results

Lemmas and a theorem are shown with respect to the sets of (21).

Lemma 1: $\tilde{\mathcal{R}}_{01} \neq \emptyset$ is equivalent to $-1 < \tilde{a}$. Then,

$$\tilde{\mathcal{R}}_{01} = \begin{cases} \{\ x \mid -1 \le x < \tilde{a}\ \} & \text{for } \tilde{a} \le 1 \\ \{\ x \mid -1 \le x \le 1\ \} & \text{for } \tilde{a} > 1 \end{cases}. \tag{22}$$

Proof. (22) is trivial from $\tilde{\mathcal{R}}_1 = \{x | x < \tilde{a}\}$ of (20). □

Lemma 2: Eq. $\tilde{f}_2(x) = 0$ has two real roots

$$\tilde{e}_2 := \frac{\tilde{a} + \tilde{b} - \sqrt{(\tilde{a} - \tilde{b})^2 + 4\tilde{d}^2}}{2} \tag{23}$$

and

$$\tilde{e}_2' := \frac{\tilde{a} + \tilde{b} + \sqrt{(\tilde{a} - \tilde{b})^2 + 4\tilde{d}^2}}{2}, \tag{24}$$

where it holds that

$$\tilde{e}_2 \le \tilde{a},\ \tilde{b} \le \tilde{e}_2. \tag{25}$$

Proof. Since $\tilde{f}_2(x) = 0$ is rewritten as $x^2 - (\tilde{a} + \tilde{b})x + \tilde{a}\tilde{b} - \tilde{d} = 0$, it is obvious that $\tilde{e}_2$ and $\tilde{e}_2'$ are the roots of this equation. The inequalities of $\tilde{e}_2 \le \tilde{a} \le \tilde{e}_2'$ in (25) are proved by

$$\tilde{a} - \tilde{e}_2 = \frac{(\tilde{a} - \tilde{b}) + \sqrt{(\tilde{a} - \tilde{b})^2 + 4\tilde{d}^2}}{2} \ge 0$$

$$\tilde{a} - \tilde{e}_2' = \frac{(\tilde{a} - \tilde{b}) - \sqrt{(\tilde{a} - \tilde{b})^2 + 4\tilde{d}^2}}{2} \le 0.$$

The inequalities $\tilde{e}_2 \le \tilde{b} \le \tilde{e}_2'$ in (25) are easily proved by replacing $\tilde{a}$ to $\tilde{b}$ in the same procedure. □

Lemma 3: $\tilde{\mathcal{R}}_{012} \neq \emptyset$ is equivalent to $-1 < \tilde{e}_2$. Then,

$$\tilde{\mathcal{R}}_{012} = \begin{cases} \{\ x \mid -1 \le x < \tilde{e}_2\ \} & \text{for } \tilde{e}_2 \le 1 \\ \{\ x \mid -1 \le x \le 1\ \} & \text{for } \tilde{e}_2 > 1 \end{cases}. \tag{26}$$

Proof. From (20), (17) and Lemma 2, $\tilde{f}_2(x) > 0$ leads to

$$\tilde{\mathcal{R}}_2 = \{\ x \mid x < \tilde{e}_2,\ \tilde{e}_2' < x\ \}. \tag{27}$$

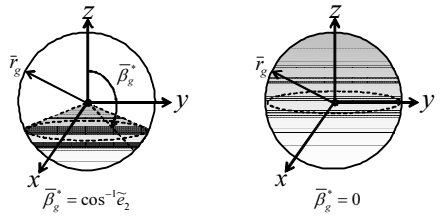

(a) The case of $-1 < \tilde{e}_2 \le 1$ (b) The case of $1 < \tilde{e}_2$

Fig. 5. The areas of the position of the COG.

Since $\tilde{\mathcal{R}}_1 = \{\ x \mid x < \tilde{a}\ \}$ and $\tilde{e}_2 \le \tilde{a} \le \tilde{e}_2'$ in (25),

$$\tilde{\mathcal{R}}_{12} := \tilde{\mathcal{R}}_1 \cap \tilde{\mathcal{R}}_2 = \{\ x \mid x < \tilde{e}_2\ \}.$$

From $\mathcal{R}_0 = \{x | -1 \le x \le 1\}$ of (19), $\tilde{\mathcal{R}}_{012} = \mathcal{R}_0 \cap \tilde{\mathcal{R}}_{12}$ of (21) is not an empty set iff $-1 < \tilde{e}_2$. Then (26) is trivial. □

Theorem 1: $\tilde{\mathcal{R}}_{0123} \neq \emptyset$ is equivalent to

$$\tilde{c} > 0, \quad -1 < \tilde{e}_2. \tag{28}$$

Then, $\tilde{\mathcal{R}}_{0123}$ is characterized by

$$\tilde{\mathcal{R}}_{0123} = \begin{cases} \{\ x \mid -1 \le x < \tilde{e}_2\ \} & \text{for } \tilde{e}_2 \le 1 \\ \{\ x \mid -1 \le x \le 1\ \} & \text{for } \tilde{e}_2 > 1 \end{cases}. \tag{29}$$

Proof. From (20), (21), (18) and Lemma 3, it is obvious that a necessary and sufficient condition is the couple of $\tilde{c} > 0$ and $-1 < \tilde{e}_2$. The set $\tilde{\mathcal{R}}_{0123}$ is obviously characterized by (29) when $\tilde{c} > 0$. □

Remark 1: The physical meaning of Theorem 1 is illustrated in Fig. 5. The position $(\bar{r}_g, \bar{\alpha}_g, \bar{\beta}_g)$ of the COG to satisfy $\tilde{\mathcal{R}}_{0123} \neq \emptyset$ is characterized as a gray subspace in the surface of the sphere with the radius $\bar{r}_g$ in the cases of (a) $-1 < \tilde{e}_2 \le 1$ and (b) $1 < \tilde{e}_2$. Note that $|\bar{\alpha}_g| \le \pi$ is arbitrary. The angle of the area is defined as

$$\bar{\beta}_g^* := \begin{cases} \cos^{-1}\tilde{e}_2 & \text{for } -1 < \tilde{e}_2 \le 1 \\ 0 & \text{for } 1 < \tilde{e}_2 \end{cases}. \tag{30}$$

In the case of (b) $1 < \tilde{e}_2$, the area of the position of the COG is the sphere. Then, the grasp is always stable with any position of the COG.

Next, let us characterize the conditions shown in Theorem 1 with respect to the normalized stiffness effects $\tilde{a}$, $\tilde{b}$ and $\tilde{d}$. From (23), the condition $-1 < \tilde{e}_2$ results in

$$(\tilde{a} + 1)(\tilde{b} + 1) > \tilde{d}^2. \tag{31}$$

Furthermore, the conditions $-1 < \tilde{e}_2 \le 1$ and $1 < \tilde{e}_2$ respectively result in

$$(\tilde{a} - 1)(\tilde{b} - 1) \le \tilde{d}^2,\ (\tilde{a} - 1)(\tilde{b} - 1) > \tilde{d}^2. \tag{32}$$

The conditions of (31) and (32) in the case of $\tilde{d}^2 < 1$ are depicted in Fig. 6. From (31) and (32), the stiffness effects $(\tilde{a}, \tilde{b}, \tilde{d})$ can be evaluated directly.

Next, let us consider a special case for $\tilde{\boldsymbol{K}}_{p\phi}$. From (9), the condition $\tilde{\boldsymbol{K}}_{p\phi} = \boldsymbol{0}$ results in

$$e = f = g = h = 0. \tag{33}$$

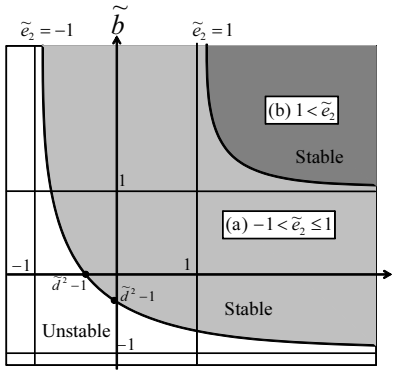

Fig. 6. The characterized areas of $\tilde{a}$ and $\tilde{b}$ in the case of $\tilde{d}^2 < 1$.

We call (33) as the decoupling condition. For preliminary, define $\mathcal{R}_{0123}$ as $\tilde{\mathcal{R}}_{0123}$ in the case of (33). And also define (e_2, e_2') as $(\tilde{e}_2, \tilde{e}_2')$ in the case of (33). From (15), (23) and (24), e_2 and e_2' are given by

$$e_2 = \frac{a+b-\sqrt{(a-b)^2+4d^2}}{2} \tag{34}$$

and

$$e_2' = \frac{a+b+\sqrt{(a-b)^2+4d^2}}{2}, \tag{35}$$

respectively. From (15) and (17), note that e_2 and e_2' are the roots of the equation $f_2(x)$ defined as

$$f_2(x) := (x-a)(x-b) - d^2. \tag{36}$$

Then, the following theorem holds with respect to $\mathcal{R}_{0123}$, (e_2, e_2') and $(\tilde{e}_2, \tilde{e}_2')$:

Theorem 2: Suppose that the decoupling condition (33) holds. $\mathcal{R}_{0123} \neq \emptyset$ is equivalent to

$$c > 0, \quad -1 < e_2. \tag{37}$$

Then, $\mathcal{R}_{0123}$ is characterized by

$$\mathcal{R}_{0123} = \begin{cases} \{\ x \mid -1 \le x < e_2\ \} & \text{for } e_2 \le 1 \\ \{\ x \mid -1 \le x \le 1\ \} & \text{for } e_2 > 1 \end{cases}. \tag{38}$$

Furthermore, for the root $\tilde{e}_2$, it holds that

$$\begin{cases} \tilde{e}_2 = e_2 & \text{for } \|\boldsymbol{\eta}\| = 0 \\ \tilde{e}_2 < e_2,\ \lim\limits_{p\to\infty} \tilde{e}_2 = e_2,\ \lim\limits_{p\to 0} \tilde{e}_2 = -\infty & \text{for } \|\boldsymbol{\eta}\| \neq 0 \end{cases}. \tag{39}$$

For the root $\tilde{e}_2'$, it also holds that

$$\begin{cases} \tilde{e}_2' = e_2' & \text{for } \|\boldsymbol{\eta}\| = 0 \\ \tilde{e}_2' < e_2',\ \lim\limits_{p\to\infty} \tilde{e}_2' = e_2',\ \lim\limits_{p\to 0} \tilde{e}_2' = e_\psi & \text{for } \|\boldsymbol{\eta}\| \neq 0 \end{cases}, \tag{40}$$

where

$$e_\psi := \frac{g^2 b + h^2 a + 2ghd}{g^2+h^2}. \tag{41}$$

Proof. From (33) and (15), c is equal to $\tilde{c}$. Therefore, Eqs. (37) and (38) obviously hold from (28) and (29).

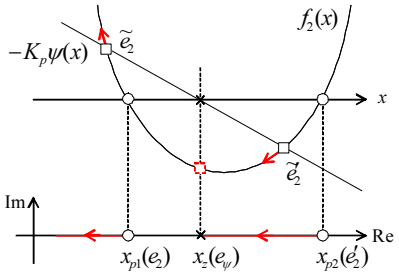

Fig. 7. The root locus of $\tilde{f}_2(x)$ with increasing K_p.

Next, consider the magnitude relation between e_2 and $\tilde{e}_2$. Suppose that $\|\boldsymbol{\eta}\| \neq 0$ since the case of $\|\boldsymbol{\eta}\| = 0$ is evident. Eq. (17) is rewritten as

$$\tilde{f}_2(x) = f_2(x) + p^{-1}\psi(x), \tag{42}$$

where $\psi(x) := (g^2+h^2)x - (g^2 b + h^2 a + 2ghd)$. Note that e_ψ of (41) is the root of $\psi(x) = 0$. The magnitude relation is evaluated by the following root locus problem:

$$K_p \frac{\psi(x)}{f_2(x)} + 1 = 0, \quad K_p := p^{-1} \tag{43}$$

where the poles x_{p_1}, x_{p_2} and the zero x_z are given by

$$x_{p_1} := e_2,\ x_{p_2} := e_2',\ x_z := e_\psi.$$

The magnitude relation between the poles and zero is analyzed as preliminaries.

$$e_2 - e_\psi = \frac{1}{2(g^2+h^2)}(l_1 - l_2), \tag{44}$$

where $l_1 := (g^2-h^2)(a-b) - 4ghd$ and $l_2 := (g^2+h^2)\sqrt{(a-b)^2+4d^2}$. It is easiliy obtained that $l_2^2 - l_1^2 \ge 0$. Eq. (44) and this fact yield to $e_2 \le e_\psi$. The inequality $e_\psi \le e_2'$ is also proved by the similar procedure because of $e_2' - e_\psi = (l_1+l_2)/\{2(g^2+h^2)\}$. Therefore, the following relationship holds:

$$e_2 \le e_\psi \le e_2' \ \Leftrightarrow\ x_{p_1} \le x_z \le x_{p_2}. \tag{45}$$

From (45) and the properties of the root locus, the root locus of (43) is depicted in Fig. 7. The lower and upper figures show the branches of the root locus in the complex plane and the behaviors of the roots expressed by the intersections of $f_2(x)$ and $-K_p\psi(x)$. The poles and zeros are represented by the circles and crosses. In the lower figure, the red arrows represent the root locus branches. It is found that the roots $\tilde{e}_2$ and $\tilde{e}_2'$ exist in the domains $(-\infty,\ e_2)$ and $(e_\psi,\ e_2')$ respectively. The roots $\tilde{e}_2$ and $\tilde{e}_2'$ start at e_2 and e_2' and approach a zero at infinity and e_ψ respectively. These facts claim the second cases of (39) and (40). □

Remark 2: The quadratic form $\boldsymbol{\eta}^{\mathrm{T}} \tilde{\boldsymbol{K}}_{pp}'^{-1} \boldsymbol{\eta}$ satisfies the inequality:

$$\frac{\|\boldsymbol{\eta}\|^2}{\lambda_{\max}} \le \boldsymbol{\eta}^{\mathrm{T}} \tilde{\boldsymbol{K}}_{pp}'^{-1} \boldsymbol{\eta} \le \frac{\|\boldsymbol{\eta}\|^2}{\lambda_{\min}}, \tag{46}$$

where $\lambda_{\min}$, $\lambda_{\max} > 0$ are the minimum and maximum eigenvalues of $\tilde{\boldsymbol{K}}_{pp}'$. Therefore, the condition $\tilde{c} > 0$ in (28)

approaches $c > 0$ in (37) by increasing the components of $\tilde{\boldsymbol{K}}'_{pp}$ against the coupling term $\boldsymbol{\eta}$.

From the properties of $\tilde{e}_2$ in (39), the relation between the characterized sets of $\mathcal{R}_{0123}$ and $\tilde{\mathcal{R}}_{0123}$ is given by

$$\tilde{\mathcal{R}}_{0123} \subseteq \mathcal{R}_{0123}. \tag{47}$$

The equality of (47) holds when $p = \Sigma_{i=1}^{n} k_{z_i}$ approaches infinity in the case of $\|\boldsymbol{\eta}\| \neq 0$. This fact in the case of $-1 < e_2,\ \tilde{e}_2 \leq 1$ is illustrated in Fig. 8, where $\bar{\beta}^*_{g1} := \cos^{-1} \tilde{e}_2$ and $\bar{\beta}^*_{g2} := \cos^{-1} e_2$.

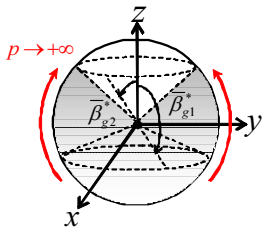

Fig. 8. The areas of the position of the COG.

IV. Conclusions

This paper considered the stable grasp from viewpoint of quasi-statics where a multi-fingered robot grasps an object by point contact. It was assumed here that each finger's grasping was regarded as a linear spring with three-DOF stiffness. Especially, this paper considered the gravity effect explicitly. The main contribution of the paper was to derive a necessary and sufficient condition for the multi-fingered grasp to be stable under the gravity effect in terms of relations among the stiffness parameters, the contact points, and the object's COG. By using the main result, it is easy to see where the object's COG should be located to guarantee the stable grasp. Furthermore, this observation shows that it is possible under a certain condition that no matter where the object's COG is located, the grasp is stable.

Assumptions 3, 4 may be difficult to establish at the initial grasp. Then to defuse these assumptions is one of our future work. In fact, there are some errors of the parameters when a hand robot grasps an object. Therefore, analysis of the parameter robustness is another future work.

References

[1] K. Shimoga, "Robot grasp synthesis algorithms: A survey," *Int. J. Robot. Res.*, vol. 15, no. 3, pp. 230–266, 1996.

[2] A. Bicchi, "Hands for dexterous manipulation and robust grasping: A difficult road toward simplicity," *IEEE Trans. Robot. Automat*, vol. 16, no. 6, pp. 652–662, 2000.

[3] D. Prattichizzo and J. Trinkle, "Grasping," in *Springer Handbook of Robotics*, B. Siciliano and O. Khatib, Eds. Springer, 2008, pp. 671–700.

[4] J. Kerr and B. Roth, "Analysis of multifingered robot hands," *Int. J. Robot. Res.*, vol. 4, no. 4, pp. 3–17, 1986.

[5] Y. Nakamura, K. Nagai, and T. Yoshikawa, "Dynamics and stability in coordination of multiple robotic mechanisms," *Int. J. Robot. Res.*, vol. 8, no. 2, pp. 44–61, 1989.

[6] T. Yoshikawa and K. Nagai, "Manipulating and grasping forces in manipulation by multifingered robot hands," *IEEE Trans. Robot. Automat.*, vol. 7, no. 1, pp. 67–77, 1991.

[7] V. Nguyen, "Constructing force-closure grasps," *Int. J. Robot. Res.*, vol. 7, no. 3, pp. 3–16, 1988.

[8] L. Magialardi, G. Mantriota, and A. Trentadue, "A three-dimensional criterion for the determination of optimal grip points," *Robot. Computer-Integrated Man.*, vol. 12, no. 2, pp. 157–167, 1996.

[9] T. Watanabe and T. Yoshikawa, "Optimization of grasping an object by using required acceleration and equilibrium-force sets," in *IEEE/ASME Int. Conf. Adv. Intel. Mech.*, 2003, pp. 338–343.

[10] A. Nakashima, T. Uno, Y. Hayakawa, T. Kondo, S. Sawada, and N. Nanba, "Synthesis of stable grasp by four-fingered robot hand for pick-and-place of assembling parts," in *5th IFAC Sym. on Mech. Sys.*, 2010, pp. 669–676.

[11] A. B. A. Cole, J. E. Hauser, and S. S. Sastry, "Kinematics and control of multifingered hands with rolling contact," *IEEE Trans. Automat. Contr.*, vol. 34, no. 4, pp. 398–404, 1989.

[12] N. Sarkar, X. Yun, and V. Kumar, "Dynamic control of 3-d rolling contacts in two-arm manipulation," *IEEE Trans. Robot. Automat.*, vol. 13, no. 3, pp. 364–376, 1997.

[13] X.-Z. Zheng, R. Nakashima, and T. Yoshikawa, "On dynamic control of finger sliding and object motion in manipulation with multifingered hands," *IEEE Trans. Robot. Automat.*, vol. 16, no. 5, pp. 469–481, 2000.

[14] K. Nagai and T. Yoshikawa, "Dynamic manipulation/grasping control of multifingered robot hands," in *IEEE Int. Conf. Robot. Automat.*, 1993, pp. 1027–1032.

[15] C. C. Cheah, H. H.-Y, S. Kawamura, and S. Arimoto, "Grasping and position control for multi-fingered robot hands with uncertain jacobian matrices," in *IEEE Int. Conf. Robot. Automat.*, 1998, pp. 2403–2408.

[16] S. Arimoto, Z. Doulgeri, P. T. A. Nguyen, and J. Fasoulas, "Stable pinching by a pair of robot fingers with soft tips under the effect of gravity," *Robotica*, vol. 20, pp. 241–249, 2002.

[17] A. Nakashima, T. Shibata, and Y. Hayakawa, "Control of grasp and manipulation by soft-finger with 3-dimensional deformation," *SICE JCMSI*, vol. 2, no. 2, pp. 78–87, 2009.

[18] S. Arimoto, *Control Theory of Mult-fingered Hands*. Springer, 2008.

[19] K. Tahara, S. Arimoto, and M. Yoshida, "Dynamic object manipulation using a virtual frame by a triple soft-fingered robotic hand," in *IEEE Int. Conf. Robot. Automat.*, 2010, pp. 4322–4327.

[20] F. Ficuciello, R. Carloni, L. Visser, and S. Stramigioli, "Port-hamiltonian modeling for soft-finger manipulation," in *IEEE/RSJ Int. Conf. Int. Robot. Sys.*, 2010, pp. 4281–4286.

[21] M. Cutkosky and I. Kao, "Computing and controlling the compliance of a robot hand," *IEEE Trans. Robot. Automat.*, vol. 5, no. 2, pp. 151–165, 1989.

[22] H. Hanafusa and H. Asada, "Stable prehension by a robot hand with elastic fingers," in *Pric. 7th Int. Symp. on Industrial Robots*, 1977, pp. 361–368.

[23] V. Nguyen, "Constructing stable grasps in 3d," in *IEEE Int. Conf. Robot. Automat.*, vol. 4, 1987, pp. 234–239.

[24] M. Kaneko, N. Imamura, K. Yokoi, and K. Tanie, "A realization of stable grasp based on virtual stiffness model by robot fingers," in *IEEE Int. Workshop on Adv. Mtn Cont.*, 1990, pp. 156–163.

[25] V. Nguyen, "Constructing stable grasps," *Int. J. Robot. Res.*, vol. 8, no. 1, pp. 26–37, 1989.

[26] T. Yamada, T. Kuraishi, Y. Mizuno, N. Mimura, and Y. Funahashi, "Stability analysis of 3d grasps by a multifingered hand," in *IEEE Int. Conf. on Robot. Automat.*, 2001, pp. 2566–2473.

[27] W. S. Howard and V. Kumar, "On the stability of grasped objects," *IEEE Trans. Robot. Automat.*, vol. 12, no. 6, pp. 904–917, 1996.

[28] D. J. Montana, "Contact stability for two-fingered grasps," *IEEE Trans. Robot. Automat.*, vol. 8, no. 4, pp. 421–430, 1992.

[29] T. Wimboeck, C. Ott, and G. Hirzinger, "Passivity-based object-level impedance control for a multifingered hand," in *IEEE/RSJ Int. Conf. Int. Robot. Sys.*, 2006, pp. 4621–4627.

[30] A. Nakashima, Y. Yoshimatsu, and Y. Hayakawa, "Analysis and synthesis of stable grasp by multi-fingered robot hand with compliance control," in *IEEE Int. Multi Conf. Sys. Cont.*, 2010, pp. 1582–1589.

[31] M. Svinin, K. Ueda, and M. Kaneko, "Analytical conditions for the rotational stability of an object in multi-finger grasping," in *IEEE Int. Conf. Robot. Automat.*, vol. 1, 1999, pp. 257 –262 vol.1.

[32] A. Nakashima and Y. Hayakawa, "Stability analysis of multi-fingered grasp under destabilizing gravity effect," in *IFAC 18th World Congress*, 2011, pp. 14 667–14 674.

[33] R. A. Horn and C. R. Johnson, *Matrix Analysis*, 2nd ed. USA: Cambridge, 2013.